

#HUTP-97/A063
10/97

Singularities of massless planar diagrams, large- N_c mesons in $3+1$ dimensions, and the 't Hooft model

Dean Lee¹
Harvard University
Cambridge, MA 02138

We study the singular Landau surfaces of planar diagrams contributing to scattering of a massless quark and antiquark in $3+1$ dimensions. In particular, we look at singularities which remain after integration with respect to the various angular degrees of freedom. We derive a general relation between these singularities and the singularities of quark-antiquark scattering in $1+1$ dimensions. We then classify all Landau surfaces of the $1+1$ dimensional system. Combining these results, we deduce that the singular surfaces of the angle-integrated $3+1$ dimensional amplitude must satisfy at least one of three conditions, which we call the planar light-cone conditions. We discuss the extension of our results to non-perturbative processes by means of the non-perturbative operator product expansion. Our findings offer new insights into the connection between the 't Hooft model and large- N_c mesons in $3+1$ dimensions and may prove useful in studies of confinement in relativistic meson systems.

1 Overview

The 't Hooft model [1], which describes large- N_c mesons in $1+1$ dimensions, is a popular starting point for studies of quark confinement in mesons. The combination of large- N_c and the low number of dimensions make it possible to calculate the Bethe-Salpeter equation exactly. Also the Bethe-Salpeter equation turns out to be relatively simple, and it is straightforward to compute the bound state wavefunctions numerically. For these reasons the 't

¹Supported by the National Science Foundation under Grant #PHY-9218167 and the Fannie and John Hertz Foundation.

Hooft model serves as a useful concrete example of confinement and relativistic bound states. Unfortunately, very little is known about the relation between confinement in the 't Hooft model and confinement in the real world. In this paper we clarify some aspects of this relation.

In our analysis we compare large- N_c massless QCD in $1 + 1$ dimensions and $3 + 1$ dimensions in terms of their corresponding Bethe-Salpeter integral kernels. Since confinement is associated with the infrared behavior of the interaction, our analysis will center on the momentum-space singularities of the Bethe-Salpeter kernel. The $3 + 1$ dimensional system carries angular degrees of freedom not in the $1 + 1$ dimensional system, and so we consider, in the $3 + 1$ dimensional case, the form of the Bethe-Salpeter kernel restricted to incoming and outgoing states with fixed intrinsic spin and orbital angular momentum. In essence we integrate the $3 + 1$ dimensional kernel, along with terms from the spherical harmonics, with respect to the angular degrees freedom.

Our work leads to two main results. The first result is that the singularities of the angle-integrated $3 + 1$ dimensional kernel, calculated to any finite number of loops, satisfy the same Landau equations that describe the singularities of the $1 + 1$ dimensional kernel. In plain terms this means that the singularities of the two kernels occur at the same place in momentum-space. The only difference is the behavior near the singularity (e.g., the two kernels may diverge with different coefficients and critical exponents). As we will see, planarity of large- N_c diagrams plays an important role in establishing this relation. The second result is the classification of all the singular surfaces of the $1 + 1$ dimensional kernel at any finite number of loops. By the first result this is also a classification of the singular surfaces of the angle-integrated $3 + 1$ dimensional kernel.

The organization of the paper is as follows. In the section 2, we provide background material on the Chisholm method for computing Feynman amplitudes. In section 3 we analyze the singularities corresponding with massless planar diagrams in $3 + 1$ dimensions and derive the first result. In section 4 examine the singularities of massless planar diagrams in $1 + 1$ dimensions and classify all possible singular surfaces, our second result. In section 5 we discuss how to apply our methods to the non-perturbative operator product expansion. In section 6 we summarize our findings and discuss their significance.

2 Chisholm method

Let \mathbf{g} be a 1PI diagram for scattering of a massless quark and antiquark, with momentum assignments as shown in Figure 1. We define $g_{(q,q');\varepsilon}^{ab;cd}(p_0)$ to be the ε -regulated amplitude of \mathbf{g} in the rest frame of p , where ε is the infinitesimal positive parameter used to regulate the singularities of the particle propagators. Since gauge-fixing affects the numerator of the gauge propagator rather than the singularities associated with the denominator, our method of gauge fixing will not affect our analysis. To avoid unnecessary abstract language, however, we will work in a covariant gauge. Ultraviolet regularization and renormalization also do not play a role in the analysis. We know this because the theory we are considering is renormalizable, and all counterterms are proportional to the original vertex interactions. Diagrams with counterterms and diagrams without counterterms therefore generate the same momentum-space singularities.

Let n be the number of internal lines and L be the number of loops in \mathbf{g} . Each gauge propagator has terms proportional to $\frac{g^{\mu\nu}}{k_j^2+i\varepsilon}$ and $\frac{k_j^\mu k_j^\nu}{(k_j^2+i\varepsilon)^2}$. We treat these terms separately when combining denominators by the Feynman parameter method. If n' is the number of gauge propagators there are $2^{n'}$ choices for the various terms, and we use the index $f = 1, \dots, 2^{n'}$ to denote a particular choice. For each f let m_f be the total number of terms proportional to $\frac{k_j^\mu k_j^\nu}{(k_j^2+i\varepsilon)^2}$. We can write the amplitude as

$$g_{(q,q');\varepsilon}^{ab;cd}(p_0) = \sum_{f=1}^{2^{n'}} \int_{\alpha \in \sigma^n} \frac{d^n \alpha \, d^{4L} l \, P_f^{ab;cd}(p_0, q, q', l, \alpha)}{\left[\sum_{j=1}^n \alpha_j k_j^2 + i\varepsilon \right]^{n+m_f}}, \quad (1)$$

where each $P_f^{ab;cd}(p_0, q, q', l, \alpha)$ is a polynomial, $\sigma^n = \left\{ \alpha \left| \alpha_j \geq 0, \sum_j \alpha_j = 1 \right. \right\}$, and for each internal line $j = 1, \dots, n$, k_j is the momentum flowing through line j .

Our purpose is to study the singular points of $g_{(q,q');\varepsilon}^{ab;cd}(p_0)$. In particular, we are interested in the singular surfaces which remain after integration with respect to the angular variables \hat{q} and \hat{q}' . Although the polynomial $P_f^{ab;cd}$ affects the behavior of $g_{(q,q');\varepsilon}^{ab;cd}(p_0)$ near the singular surfaces, the structure of

the surfaces is determined by the zero-set of the denominator,

$$\sum_{j=1}^n \alpha_j k_j^2 + i\varepsilon. \quad (2)$$

In some sense the singular points of $g_{(q,q');\varepsilon}^{ab;cd}(p_0)$ are a subset of the singular points of the function

$$g_\varepsilon(p_0, q, q') = \int_{\alpha \in \sigma^n} \frac{d^n \alpha \, d^{4L} l}{\left[\sum_{j=1}^n \alpha_j k_j^2 + i\varepsilon \right]^n} \propto \int d^{4L} l \prod_{j=1}^n \frac{1}{k_j^2 + i\varepsilon}. \quad (3)$$

In more precise terms, each singular point of $g_{(q,q');\varepsilon}^{ab;cd}(p_0)$ is a solution of the Landau equations¹ of $g_\varepsilon(p_0, q, q')$. These two statements can differ when a solution of the Landau equations of $g_\varepsilon(p_0, q, q')$ is a regular point of $g_\varepsilon(p_0, q, q')$ as a result of accidental cancellation.

Throughout the rest of this section, we consider the singular points of

$$g_{\vec{\varepsilon}}(p_0, q, q') = \int_{\alpha \in \sigma^n} \frac{d^n \alpha \, d^{4L} l}{\left[\sum_{j=1}^n \alpha_j (k_j^2 + i\varepsilon_j) \right]^n} \propto \int d^{4L} l \prod_{j=1}^n \frac{1}{k_j^2 + i\varepsilon_j}. \quad (4)$$

For convenience later on we have generalized our infinitesimal parameter ε to a vector of infinitesimal parameters $\vec{\varepsilon} = \{\varepsilon_1, \dots, \varepsilon_n\}$. For each loop i and internal line j , let

$$Z_{ij} = \begin{cases} 1 & \text{if loop } i \text{ contains line } j \text{ with orientation } k_j \\ -1 & \text{if loop } i \text{ contains line } j \text{ with orientation } -k_j \\ 0 & \text{if loop } i \text{ does not contain line } j. \end{cases} \quad (5)$$

We can perform the loop integrations [2] to get

$$g_{\vec{\varepsilon}}(p_0, q, q') = \int_{\alpha \in \sigma^n} \frac{d^n \alpha \, [C(\alpha)]^{n-2L-2}}{\left[\sum_{\substack{h=p^2, q^2, q'^2, \\ p \cdot q, p \cdot q', q \cdot q'}} h D_h(\alpha) + iC(\alpha) \sum_{j=1}^n \alpha_j \varepsilon_j \right]^{n-2L}}, \quad (6)$$

¹The Landau equations are written out in equations (39) and (40) of the next section.

where each $D_h(\alpha)$ is a homogeneous polynomial of degree $L+1$, and $C(\alpha)$ is a homogeneous polynomial of degree L . We have dropped various constant factors which will be irrelevant to our discussion. $C(\alpha)$ can be written in determinant form:²

$$C(\alpha) = \det \mathbf{C} = \begin{vmatrix} a_{1,1} & \cdots & a_{1,L} \\ \vdots & \ddots & \vdots \\ a_{L,1} & \cdots & a_{L,L} \end{vmatrix} \quad (7)$$

where $a_{i,i'} = \sum_j \alpha_j Z_{ij} Z_{i'j}$. For each internal line $j = 1, \dots, n$, let \dot{k}_j be the momentum flowing through line j when all independent loop momenta are set to zero. We can write $\sum_{h=p^2, q^2, q'^2, p \cdot q, p \cdot q', q \cdot q'} h D_h(\alpha)$ as a symbolic determinant:

$$\sum_{h=p^2, q^2, q'^2, p \cdot q, p \cdot q', q \cdot q'} h D_h(\alpha) = \begin{vmatrix} a_{1,1} & \cdots & a_{1,L} & a_{1,L+1} \\ \vdots & \ddots & \vdots & \vdots \\ a_{L,1} & \cdots & a_{L,L} & a_{L,L+1} \\ a_{L+1,1} & \cdots & a_{L+1,L} & a_{L+1,L+1} \end{vmatrix} \quad (8)$$

where for $1 \leq i \leq L$, $a_{i,L+1} = a_{L+1,i} = \sum_j Z_{ij} \alpha_j \dot{k}_j^\mu$, and $a_{L+1,L+1} = \sum_{i,j} (Z_{ij})^2 \alpha_j \dot{k}_j^2$.

In our definition of the symbolic determinant, we identify the product $a_{i,L+1} a_{i',L+1}$, for $1 \leq i, i' \leq L$, with the corresponding Lorentz contraction:

$$\left(\sum_j Z_{ij} \alpha_j \dot{k}_j^\mu \right) \left(\sum_j Z_{i'j} \alpha_j \dot{k}_{j\mu} \right). \quad (9)$$

Let us consider the angular integral

$$G_{\vec{\varepsilon}} \left(\frac{p_0, q_0, q'_0}{|\vec{q}|, |\vec{q}'|} \right) = \frac{1}{8\pi^2} \int d\cos\theta_{\hat{q},\hat{z}} d\cos\theta_{\hat{q},\hat{q}'} d\phi_{\hat{q},\hat{z}} d\phi_{\hat{q},\hat{q}'} \vec{q}^2 \vec{q}'^2 g_{\vec{\varepsilon}}(p_0, q, q'), \quad (10)$$

where $\theta_{\hat{q},\hat{z}}$ is the angle between \hat{q} and the z -axis, $\phi_{\hat{q},\hat{z}}$ is the azimuthal angle of \hat{q} about the z -axis, $\theta_{\hat{q},\hat{q}'}$ is the angle between \hat{q} and \hat{q}' , $\phi_{\hat{q},\hat{q}'}$ is the azimuthal angle of \hat{q} about \hat{q}' . Since we are in the rest frame where $\vec{p} = 0$, all Lorentz invariants in the denominator of (6) are independent of these angular variables with the exception of $q \cdot q'$, which is given by

$$q \cdot q' = q_0 q'_0 - |\vec{q}| |\vec{q}'| \cos\theta_{\hat{q},\hat{q}'} \quad (11)$$

²See [3].

We can rewrite (10) as

$$G_{\vec{\varepsilon}} = \int_{\alpha \in \sigma^n} d^n \alpha \int \frac{d \cos \theta_{\hat{q}, \hat{q}'} [C(\alpha)]^{n-2L-2} \vec{q}^2 \vec{q}'^2}{\left[\sum_{\substack{h=p^2, q^2, q'^2, \\ p \cdot q, p \cdot q', q \cdot q'}} h D_h(\alpha) + i C(\alpha) \sum_{j=1}^n \alpha_j \varepsilon_j \right]^{n-2L}}. \quad (12)$$

Integrating with respect to $\cos \theta_{\hat{q}, \hat{q}'}$, we find $G_{\vec{\varepsilon}}$ equals

$$\sum_{\lambda=-1, +1} \int_{\alpha \in \sigma^n} \frac{d^n \alpha \frac{1}{(n-2L-1)D_{q \cdot q'}(\alpha)} \lambda [C(\alpha)]^{n-2L-2} |\vec{q}| |\vec{q}'|}{\left[\sum_{\substack{h=p^2, q^2, q'^2, \\ p \cdot q, p \cdot q', q \cdot q'}} h D_h(\alpha) + (q_0 q'_0 - \lambda |\vec{q}| |\vec{q}'|) D_{q \cdot q'}(\alpha) + i C(\alpha) \sum_{j=1}^n \alpha_j \varepsilon_j \right]^{n-2L-1}} \quad (13)$$

3 Planar diagrams

Let us now restrict to the case when \mathfrak{g} is a planar diagram. As an example, let us consider the diagram shown in Figure 2. It is convenient to route our loop momentum variables such that each independent loop circumscribes a region (i.e., tile) of our planar diagram. In our example we take k_2 and k_6 to be the independent loop momenta. With this convention \dot{k}_j is then defined by setting $k_2 = k_6 = 0$. For this diagram, $\sum_{\substack{h=p^2, q^2, q'^2, \\ p \cdot q, p \cdot q', q \cdot q'}} h D_h(\alpha)$ is given by

$$\sum_{\substack{h=p^2, q^2, q'^2, \\ p \cdot q, p \cdot q', q \cdot q'}}$$

$$\begin{vmatrix} \alpha_1 + \alpha_2 + \alpha_3 + \alpha_4 & -\alpha_4 & \alpha_3 \dot{k}_3 + \alpha_4 \dot{k}_4 + \alpha_1 \dot{k}_1 \\ -\alpha_4 & \alpha_4 + \alpha_5 + \alpha_6 + \alpha_7 & \alpha_7 \dot{k}_7 - \alpha_4 \dot{k}_4 + \alpha_5 \dot{k}_5 \\ \alpha_3 \dot{k}_3 + \alpha_4 \dot{k}_4 + \alpha_1 \dot{k}_1 & \alpha_7 \dot{k}_7 - \alpha_4 \dot{k}_4 + \alpha_5 \dot{k}_5 & a_{33} \end{vmatrix} \quad (14)$$

where

$$\begin{aligned} 2\dot{k}_1 &= p + q' \\ 2\dot{k}_3 &= p + q \\ 2\dot{k}_4 &= 2p \\ 2\dot{k}_5 &= -p + q \\ 2\dot{k}_7 &= -p + q' \end{aligned} \quad (15)$$

and

$$a_{33} = \alpha_1 \dot{k}_1^2 + \alpha_3 \dot{k}_3^2 + \alpha_4 \dot{k}_4^2 + \alpha_5 \dot{k}_5^2 + \alpha_7 \dot{k}_7^2. \quad (16)$$

We find that $D_{q \cdot q'}(\alpha)$ equals

$$-\frac{1}{2} [\alpha_1 \alpha_3 (\alpha_4 + \alpha_5 + \alpha_6 + \alpha_7) + \alpha_5 \alpha_7 (\alpha_1 + \alpha_2 + \alpha_3 + \alpha_4) + (\alpha_1 \alpha_5 + \alpha_3 \alpha_7) \alpha_4]. \quad (17)$$

There is a correspondence between the terms in $D_{q \cdot q'}(\alpha)$ and paths from the left-side of \mathbf{g} to the right-side of \mathbf{g} .³ We define a path to be a continuous walk through adjacent interior regions such that no region is entered twice. We have shown all possible left-to-right paths for \mathbf{g} in Figures 2(a-d). For each path ρ , let $|\rho|$ be the total number of internal lines crossed. We use an alternating string of α 's and l 's,

$$\left\{ \alpha_{j_1(\rho)}, l_{i_1(\rho)}, \dots, \alpha_{j_{|\rho|-1}(\rho)}, l_{i_{|\rho|-1}(\rho)} \alpha_{j_{|\rho|}(\rho)} \right\}, \quad (18)$$

to denote the sequence of internal lines crossed and loop regions entered by ρ . With each string we associate the polynomial

$$\alpha_{j_1(\rho)} \alpha_{j_2(\rho)} \cdots \alpha_{j_{|\rho|}(\rho)} C(\alpha, i_1(\rho), \dots, i_{|\rho|-1}(\rho)), \quad (19)$$

where $C(\alpha, i_1(\rho), \dots, i_{|\rho|}(\rho))$ is the determinant of the submatrix generated by striking out the $i_1(\rho), \dots, i_{|\rho|}(\rho)$ rows and columns of the matrix \mathbf{C} shown in equation (7). When $|\rho| - 1 = L$, we take $C(\alpha, i_1(\rho), \dots, i_{|\rho|-1}(\rho)) = 1$. The expression for $D_{q \cdot q'}(\alpha)$ is then

$$D_{q \cdot q'}(\alpha) = -\frac{1}{2} \sum_{\text{paths } \rho} \alpha_{j_1(\rho)} \alpha_{j_2(\rho)} \cdots \alpha_{j_{|\rho|}(\rho)} C(\alpha, i_1(\rho), \dots, i_{|\rho|-1}(\rho)). \quad (20)$$

When $\alpha_j \geq 0$ for each j , we find $D_{q \cdot q'}(\alpha) \leq 0$. In fact $D_{q \cdot q'}(\alpha) \leq 0$ for any planar diagram since $C(\alpha, i_1(\rho), \dots, i_{|\rho|-1}(\rho))$ is the determinant of a positive quadratic form. Under the constraint $\alpha_j \geq 0$ for each j , we can use our correspondence with left-to-right paths to conclude that $D_{q \cdot q'}(\alpha) = 0$ if and only if there exists j'_1, \dots, j'_r such that

$$\alpha_{j'_1} = \alpha_{j'_2} = \cdots = \alpha_{j'_r} = 0 \quad (21)$$

³This correspondence is proven in [3].

and for every left-to-right path ρ ,

$$\{j_1(\rho), \dots, j_{|\rho|}(\rho)\} \cap \{j'_1, \dots, j'_r\} \neq \emptyset. \quad (22)$$

Let $-\frac{1}{2}\alpha_{j_1}\alpha_{j_2}\cdots\alpha_{j_{L+1}}$ be any monomial appearing in $D_{q\cdot q'}(\alpha)$. Taking successive derivatives of $G_{\bar{\varepsilon}}$ with respect to $\varepsilon_{j_1}, \varepsilon_{j_2}, \dots, \varepsilon_{j_{L+1}}$ we find $\frac{d}{d\varepsilon_{j_1}} \cdots \frac{d}{d\varepsilon_{j_{L+1}}} G_{\bar{\varepsilon}}$ is proportional to

$$\sum_{\lambda=-1,+1} \int_{\alpha \in \sigma^n} \frac{d^n \alpha \frac{\alpha_{j_1}\alpha_{j_2}\cdots\alpha_{j_{L+1}} i^{L+1}}{(n-2L-1)D_{q\cdot q'}(\alpha)} \lambda [C(\alpha)]^{n-L-1} |\vec{q}| |\vec{q}'|}{\left[\sum_{\substack{h=p^2, q^2, q'^2, \\ p\cdot q, p\cdot q'}} h D_h(\alpha) + (q_0 q'_0 - \lambda |\vec{q}| |\vec{q}'|) D_{q\cdot q'}(\alpha) + i \sum_{j=1}^n \alpha_j \varepsilon_j \cdot C(\alpha) \right]^{n-L}}. \quad (23)$$

We recall that $D_{q\cdot q'}(\alpha)$ is a sum of monomials each with negative coefficient. Since one of these monomials is $-\frac{1}{2}\alpha_{j_1}\alpha_{j_2}\cdots\alpha_{j_{L+1}}$,

$$D_{q\cdot q'}(\alpha) \leq -\frac{1}{2}\alpha_{j_1}\alpha_{j_2}\cdots\alpha_{j_{L+1}} \leq 0 \quad (24)$$

for all $\alpha \in \sigma^n$. We conclude that $\frac{\alpha_{j_1}\alpha_{j_2}\cdots\alpha_{j_{L+1}}}{D_{q\cdot q'}(\alpha)}$ is analytic on the interior of σ^n and bounded on σ^n .

Let us now consider the singular points of $\frac{d}{d\varepsilon_{j_1}} \cdots \frac{d}{d\varepsilon_{j_{L+1}}} G_{\bar{\varepsilon}} \Big|_{\varepsilon_1 = \dots = \varepsilon_n = \varepsilon}$. We can simplify matters by considering the singular points of the related function F_{ε} , which we get by removing some of the analytic factors in the numerator of (23):

$$\sum_{\lambda=-1,+1} \int_{\alpha \in \sigma^n} \frac{d^n \alpha [C(\alpha)]^{n-L-1}}{\left[\sum_{\substack{h=p^2, q^2, q'^2, \\ p\cdot q, p\cdot q'}} h D_h(\alpha) + (q_0 q'_0 - \lambda |\vec{q}| |\vec{q}'|) D_{q\cdot q'}(\alpha) + i\varepsilon \cdot C(\alpha) \right]^{n-L}}. \quad (25)$$

Comparing (25) with the Chisholm result in (6), we observe that F_{ε} is the $1+1$ dimensional analog of $g_{\varepsilon}(p_0, q, q')$.⁴ By this we mean

$$F_{\varepsilon} \propto \int d^{2L} l \prod_{j=1}^n \frac{1}{k_j^{\sharp 2} + i\varepsilon} + \int d^{2L} l \prod_{j=1}^n \frac{1}{k_j^{\flat 2} + i\varepsilon}, \quad (26)$$

⁴In $1+1$ dimensions, the exponent of the numerator in (6) is $n-L-1$, and the exponent of the denominator is $n-L$.

where k_j^\sharp and k_j^b are Lorentz vectors in 1+1 dimensions with the identifications

$$p^{\sharp\mu} = p^b\mu = (p_0, 0); \quad (27)$$

$$q^{\sharp\mu} = q^b\mu = (q_0, |\vec{q}|); \quad (28)$$

$$q'^{\sharp\mu} = (q'_0, |\vec{q}'|); \quad q'^b\mu = (q'_0, -|\vec{q}'|). \quad (29)$$

We conclude that for each monomial $\alpha_{j_1}\alpha_{j_2}\cdots\alpha_{j_{L+1}}$ appearing in $D_{q\cdot q'}(\alpha)$, the singular points of $\frac{d}{d\varepsilon_{j_1}}\cdots\frac{d}{d\varepsilon_{j_{L+1}}}G_{\vec{\varepsilon}}\Big|_{\varepsilon_1=\cdots=\varepsilon_n=\varepsilon}$ satisfy the 1+1 dimensional Landau equations for F_ε .

Let us now suppose $G_{\vec{\varepsilon}}\Big|_{\varepsilon_1=\cdots=\varepsilon_n=\varepsilon}$ has a singular point that does not satisfy the Landau equations of F_ε . From our conclusion regarding the derivatives of $G_{\vec{\varepsilon}}$, we deduce that the singularities of $G_{\vec{\varepsilon}}\Big|_{\varepsilon_1=\cdots=\varepsilon_n=\varepsilon}$ must have the form

$$\sum_\eta s_\eta(\varepsilon_{j_1(\eta)}, \dots, \varepsilon_{j_{n(\eta)}(\eta)}) \Bigg|_{\varepsilon_1=\cdots=\varepsilon_n=\varepsilon} \quad (30)$$

where for each η and each monomial $\alpha_{\bar{j}_1}\alpha_{\bar{j}_2}\cdots\alpha_{\bar{j}_{L+1}}$ appearing in $D_{q\cdot q'}(\alpha)$, there exists $\bar{j}_i \notin \{j_1(\eta), \dots, j_{n(\eta)}(\eta)\}$. Let us consider one such term

$$s_\eta(\varepsilon_{j_1(\eta)}, \dots, \varepsilon_{j_{n(\eta)}(\eta)}). \quad (31)$$

Since s_η is independent of some of the ε_j , its singularities are due to a contracted version of the diagram \mathfrak{g} , where the propagators $\frac{1}{k_j^2 + i\varepsilon_j}$ corresponding with internal lines $j \notin \{j_1(\eta), \dots, j_{n(\eta)}(\eta)\}$ have been removed. We define a new function $\tilde{g}_{\vec{\varepsilon}}$ which corresponds with this contracted version of $g_{\vec{\varepsilon}}$:

$$\tilde{g}_{\vec{\varepsilon}}(p_0, q, q') = \int d^{4L}l \prod_{r=1}^{n(\eta)} \frac{1}{k_{j_r(\eta)}^2 + i\varepsilon_{j_r(\eta)}}. \quad (32)$$

Performing the loop integrations, we get

$$\tilde{g}_{\vec{\varepsilon}}(p_0, q, q') = \int_{\alpha \in \sigma^{n(\eta)}} \frac{d^{n(\eta)}\alpha \left[\tilde{C}(\alpha) \right]^{n(\eta)-2L-2}}{\left[\sum_{\substack{h=p^2, q^2, q'^2, \\ p\cdot q, p\cdot q', q\cdot q'}} h \tilde{D}_h(\alpha) + i\tilde{C}(\alpha) \sum_{r=1}^{n(\eta)} \alpha_{j_r(\eta)} \varepsilon_{j_r(\eta)} \right]^{n(\eta)-2L}}, \quad (33)$$

where

$$\sigma^{n(\eta)} = \left\{ \alpha \left| \alpha_j \geq 0, \sum_j \alpha_j = 1, \alpha_j = 0 \text{ when } j \notin \{j_r(\eta)\}_{r=1}^{n(\eta)} \right. \right\}. \quad (34)$$

We define $\tilde{G}_{\tilde{\varepsilon}}$ in the same manner as G_{ε} :

$$\tilde{G}_{\tilde{\varepsilon}} \left(\frac{p_0, q_0, q'_0}{|\vec{q}|, |\vec{q}'|} \right) = \frac{1}{8\pi^2} \int d \cos \theta_{\hat{q}, \hat{z}} d \cos \theta_{\hat{q}, \hat{q}'} d \phi_{\hat{q}, \hat{z}} d \phi_{\hat{q}, \hat{q}'} \vec{q}^2 \vec{q}'^2 \tilde{g}_{\tilde{\varepsilon}}(p_0, q, q'). \quad (35)$$

The singular points of $s_{\eta}|_{\varepsilon_1 = \dots = \varepsilon_n = \varepsilon}$ must satisfy the Landau equations for $\tilde{G}_{\tilde{\varepsilon}}|_{\varepsilon_1 = \dots = \varepsilon_n = \varepsilon}$. We note, however, that $\tilde{D}_{q, q'}(\alpha) = 0$ for all $\alpha \in \sigma^{n(\eta)}$. $\tilde{g}_{\tilde{\varepsilon}}(p_0, q, q')$ is therefore independent of all the angular variables and there is a direct relationship between the singularities of $\tilde{G}_{\tilde{\varepsilon}}|_{\varepsilon_1 = \dots = \varepsilon_n = \varepsilon}$ and the singularities of the corresponding contracted diagram in $1+1$ dimensions:

$$\tilde{F}_{\varepsilon} = \int d^{2L} l \prod_{r=1}^{m(\eta)} \frac{1}{k_{j_r(\eta)}^{\sharp 2} + i\varepsilon} = \int d^{2L} l \prod_{r=1}^{m(\eta)} \frac{1}{k_{j_r(\eta)}^{\flat 2} + i\varepsilon}. \quad (36)$$

The singular points of $\tilde{G}_{\tilde{\varepsilon}}|_{\varepsilon_1 = \dots = \varepsilon_n = \varepsilon}$, and therefore $s_{\eta}|_{\varepsilon_1 = \dots = \varepsilon_n = \varepsilon}$, must satisfy the Landau equations for \tilde{F}_{ε} (in this case, no angular integrations are required). But the Landau equations for \tilde{F}_{ε} are a subset of the Landau equations for F_{ε} , which contradicts our supposition. We conclude that all singular points of $G_{\tilde{\varepsilon}}|_{\varepsilon_1 = \dots = \varepsilon_n = \varepsilon}$ satisfy the Landau equations for F_{ε} .

These results can be generalized to show that for any nonnegative integer r , the singular points of

$$\frac{1}{8\pi^2} \int d \cos \theta_{\hat{q}, \hat{z}} d \cos \theta_{\hat{q}, \hat{q}'} d \phi_{\hat{q}, \hat{z}} d \phi_{\hat{q}, \hat{q}'} (\cos \theta_{\hat{q}, \hat{q}'})^r \vec{q}^2 \vec{q}'^2 g_{\varepsilon}(p_0, q, q') \quad (37)$$

must also satisfy the Landau equations for F_{ε} . When $r > 0$, the argument involving s_{η} is altered slightly. Instead of s_{η} being independent of some of the ε_j 's, s_{η} is now a polynomial of degree $\leq r$ with respect to these ε_j 's. The arguments that follow, however, are identical with that of the $r = 0$ case.

4 Landau surfaces in $1+1$ dimensions

We examine the Landau equations for $g_\varepsilon(p_0, q, q')$ in $1+1$ dimensions, where

$$g_\varepsilon(p_0, q, q') = \int_{\alpha \in \sigma^n} \frac{d^n \alpha \, d^{2L} l}{\left[\sum_{j=1}^n \alpha_j k_j^2 + i\varepsilon \right]^n} \propto \int d^{2L} l \prod_{j=1}^n \frac{1}{k_j^2 + i\varepsilon}. \quad (38)$$

Let $\bar{p}^0, \bar{q}, \bar{q}'$ be a singular point of g_ε . There must exist some configuration of the Feynman parameters $\bar{\alpha}_j \in \sigma^n$ and internal momenta \bar{k}_j^μ satisfying the Landau equations for g_ε , which we state as follows.⁵ For each internal line j ,

$$\bar{\alpha}_j = 0 \quad \text{or} \quad \bar{k}_j^2 = 0 \quad (39)$$

and for any closed loop i ,

$$\sum_j Z_{ij} \bar{\alpha}_j \bar{k}_j^\mu = 0, \quad (40)$$

where $Z_{ij} = \pm 1$ is the relative orientation of i and \bar{k}_j^μ . We now fix the values of $\bar{\alpha}_j$ and \bar{k}_j^μ for the rest of our discussion. Let us define a new diagram \mathbf{g}' , which we construct by contracting all internal lines j of \mathbf{g} such that $\bar{\alpha}_j = 0$ or $\bar{k}_j^\mu = 0$. We mention that \mathbf{g}' differs from the standard notion for a contracted diagram of \mathbf{g} , where one contracts lines satisfying the single condition $\bar{\alpha}_j = 0$. To avoid confusion, we call \mathbf{g}' the doubly-contracted diagram of \mathbf{g} . In the following we assume that \mathbf{g}' has at least two vertices.

We now add some extra names and markings to the internal lines of \mathbf{g}' . In $1+1$ dimensions all Lorentz vectors on the light-cone take the form (k_0, k_0) or $(k_0, -k_0)$ for some real k_0 . For each internal line j of \mathbf{g}' we call j a type I line if $\bar{k}_j^\mu = (\bar{k}_{j0}, \bar{k}_{j0})$ and call j a type II line if $\bar{k}_j^\mu = (\bar{k}_{j0}, -\bar{k}_{j0})$. For each type I line we draw a single arrowhead, oriented such that the time-component is positive. We do the same with each type II line, except this time using a double arrowhead. We have illustrated the use of these markings in Figures 3(a-b). Let v_1 and v_2 be vertices of \mathbf{g}' . If there exists a continuous path along type I (II) lines from v_1 to v_2 , ignoring for the moment the direction of the

⁵We are considering a completely massless theory, and the problem of new singularities at infinite loop momenta (sometimes referred to as second-type singularities) does not occur.

arrowheads, then we say that v_1 and v_2 are I-connected (II-connected). If there exists a continuous path along type I (II) lines from v_1 to v_2 following along the direction of the arrowheads, then we say that v_1 is I-trajected (II-trajected) to v_2 . We now prove some results that follow from the Landau equations.

Proposition 1 *No vertex is I-trajected (II-trajected) to itself.*

Proof: Suppose that there existed such an I-trajectory. Let $\bar{k}_1^\mu, \dots, \bar{k}_m^\mu$ be the corresponding momenta of the lines in the trajectory. By the Landau equations $\sum_{j=1}^m \bar{\alpha}_j \bar{k}_j^\mu = 0$. This, however, contradicts the fact that each $\bar{\alpha}_j$ and \bar{k}_j^0 is positive. \diamond

Proposition 2 *If v_1 is I-trajected (II-trajected) to v_2 , then v_1 and v_2 are not II-connected (I-connected).*

Proof: Suppose v_1 is I-trajected to v_2 , and v_1 and v_2 are II-connected. Let us consider the closed loop consisting of an I-trajectory from v_1 to v_2 followed by a II-connected path from v_2 to v_1 . We write the momenta of the I-trajectory as $\bar{k}_1^\mu, \dots, \bar{k}_m^\mu$ and the momenta of the II-connected path as $\bar{k}_{m+1}^\mu, \dots, \bar{k}_n^\mu$. From the Landau equations,

$$\sum_{j=1}^m \bar{\alpha}_j \bar{k}_j^\mu = - \sum_{j=m+1}^n \bar{\alpha}_j \bar{k}_j^\mu. \quad (41)$$

The Lorentz vector on the left-side of (41) is non-zero since each $\bar{\alpha}_j$ and \bar{k}_j^0 is positive. But this leads to a contradiction since the left-side must be parallel to the vector $(1, 1)$ while the right-hand side must be parallel to $(1, -1)$. \diamond

Since type I vectors and type II vectors are linearly independent, the constraint of momentum conservation at any internal vertex, v , requires separate conservation of type I vectors and type II vectors. In particular this means that if there is a type I (II) vector entering v there must also be a type I (II) vector leaving v and vice-versa. We point out that these statements are not true of external vertices.

The relation of I-connectivity (II-connectivity) divides the vertices of \mathfrak{g}' into equivalence classes, which we call I-connected (II-connected) components. We now prove the following result.

Proposition 3 *Each I-connected (II-connected) component contains at least two external vertices.*

Proof: Let v be an external vertex and let us suppose that v is the only external vertex in the I-connected component containing v . v must have a type I vector leaving or entering it. Without loss of generality, we assume that there is a type I vector leaving v and entering a new vertex which we call v_1 . Let us now consider the I-trajectory from v to v_1 . Since v_1 is an internal vertex, there must also be a type I vector leaving v_1 . We can extend the I-trajectory in this manner. By Proposition 1 we never enter the same vertex twice, and since v is the only external vertex in our I-connected component we can extend the I-trajectory indefinitely. This contradicts the fact that \mathfrak{g}' is finite.

Let us now suppose v is an internal vertex and the I-connected component containing v has no external vertices. We again consider I-trajectories starting from v and find the contradiction that the I-trajectory can be extended indefinitely. \diamond

A simple extension of the argument of the last proof gives us the result that each I-connected (II-connected) component must contain two external vertices, v_1 and v_2 such that v_1 is I-trajected (II-trajected) to v_2 . Using this result and Propositions 2 and 3, we find that the I-connected and II-connected components of \mathfrak{g}' must have the one of the configurations shown in Figures 4(a-h). We have omitted diagrams related to the ones shown by switching I and II or permuting the external lines. The topology of these diagrams provides a good deal of information about the structure of the corresponding Landau surface. One obvious but useful observation is that if there is a way to cut \mathfrak{g}' into two pieces such that each cut line is of the same type, the momentum flowing across the cut must be a Lorentz vector of that type. For example the Landau surface associated with the diagram in Figure 4(a) is given by $k^0 = k^1 \neq 0$, where k^μ is the momentum flowing through the diagram. Examining the structure of each of the diagrams in Figures 4(a-h), we conclude that the Landau surfaces for any planar 1 + 1 dimensional massless diagram must satisfy one the following properties: (i) one of the external quark or antiquark lines is light-like; (ii) the total momentum p is light-like (we are using the momentum assignments shown in Figure 1); or (iii) the total t -channel momentum $\frac{q-q'}{2}$ is light-like.⁶ This is the central

⁶In contrast with the previous section, the methods used in this section do not require

result of our analysis, and for future reference we will call these conditions the planar light-cone conditions.

Before closing this section we mention that in addition to the diagrams shown in Figures 4(a-h), it is also possible that \mathfrak{g}' consists of a single point without any internal lines. The Landau surface associated with this diagram, however, is merely a set of special limit points on the Landau surfaces associated with the other diagrams. For example, this includes the point $k^\mu = 0$, where k^μ is the momentum flowing through the diagram in Figure 4(a).

5 Non-perturbative OPE

Our analysis and results can be extended to non-perturbative phenomena by means of the non-perturbative operator product expansion. In this version of the operator product expansion one considers, in addition to the usual perturbative terms, quantities proportional to vacuum condensates of various local operators.⁷ It is believed that such vacuum condensates are responsible for (or at least associated with) long-distance confinement phenomena. In this context the singularities we wish to study are the momentum-space singularities of the Wilson coefficients in the operator expansion. As an example we consider the Wilson coefficient of the gluon condensate $\langle :G^{\mu\nu}G_{\mu\nu}: \rangle$ for the process shown in Figure 5(a). The rectangle shown in Figure 5(a) is meant to represent the insertion of the condensate $\langle :G^{\mu\nu}G_{\mu\nu}: \rangle$. The coefficient is calculated by setting the momentum of each of the two lines touching the condensate equal to zero. The singularities of this coefficient are the same as that of the process shown in Figure 5(b), where the \times 's are meant to represent a two point interaction. In fact the singularities of any connected Wilson coefficient (i.e., one which does not produce momentum-space delta functions) are equivalent to that of a perturbative Feynman diagram with some internal lines deleted. Since the methods of our singularity analysis apply to general planar diagrams, our results apply to any connected planar Wilson coefficient. We deduce that in $3 + 1$ dimensions, the singularities of any angle-integrated, connected, planar Wilson coefficient satisfy the planar light-cone conditions.

that the diagram be planar. If the diagram is not planar, there is another possibility for the Landau surface, namely that the u -channel momentum $\frac{q+q'}{2}$ is light-like. This can be seen by twisting the top or bottom half of the diagram shown in Figure 4(h).

⁷For a discussion of the non-perturbative operator product expansion see [4].

Disconnected Wilson coefficients produce Dirac delta functions in momentum-space and for this reason we consider them separately. Fortunately the number of ways the delta function can appear is quite limited, and for any number of dimensions, the disconnected planar Wilson coefficients are non-zero only when (i') one of the external quark or antiquark lines has zero momentum; (ii') the total momentum p is zero; or (iii') the total t -channel momentum $\frac{q-q'}{2}$ is zero. We note that these conditions for the disconnected coefficients are subsets of the planar light-cone conditions as defined in section 4. We conclude that in $3 + 1$ dimensions, the singularities of any angle-integrated planar Wilson coefficient, either connected or disconnected, satisfy the planar light-cone conditions.

6 Summary and comments

We found that for massless planar diagrams the singular points of the angle-integrated amplitude,

$$\int_{\hat{q}, \hat{q}'} (\cos \theta_{\hat{q}, \hat{q}'})^r \vec{q}^2 \vec{q}'^2 g_{(q, q'); \varepsilon}^{ab; cd}(p_0), \quad (42)$$

lie along the Landau surfaces of the following $1 + 1$ dimensional analog of $g_{(q, q'); \varepsilon}^{ab; cd}(p_0)$. To each external $3 + 1$ dimensional vector e^μ we associate one or two $1 + 1$ dimensional vectors $e^{\sharp\mu}$ and $e^{\flat\mu}$, according to the rules

$$p^{\sharp\mu} = p^{\flat\mu} = (p_0, 0), \quad (43)$$

$$q^{\sharp\mu} = q^{\flat\mu} = (q_0, |\vec{q}|), \quad (44)$$

$$q'^{\sharp\mu} = (q'_0, |\vec{q}'|), \quad q'^{\flat\mu} = (q'_0, -|\vec{q}'|). \quad (45)$$

The singular points of (42) are contained in the union of the Landau surfaces of $g_{(q^\sharp, q'^\sharp); \varepsilon}^{ab; cd}(p_0)$ and $g_{(q^\flat, q'^\flat); \varepsilon}^{ab; cd}(p_0)$.

In the $1 + 1$ dimensional problem, we used the Landau equations to restrict the topology of the doubly-contracted diagram \mathfrak{g}' . These restrictions place constraints on the singular surfaces of the amplitude of the diagram. We found that the singular surfaces of any planar $1 + 1$ dimensional massless diagram must satisfy one of the following planar light-cone conditions: (i) one of the external quark or antiquark lines is light-like; (ii) the total momentum p is light-like; or (iii) the total t -channel momentum $\frac{q-q'}{2}$ is light-like. Combining

this with the first result, we conclude that the singular surfaces of the angle-integrated $3+1$ dimensional amplitude must also satisfy the planar light-cone conditions. We then applied our methods to the non-perturbative operator product expansion and obtained analogous results for the singularities of planar Wilson coefficients.

As mentioned in the introduction, confinement is associated with the infrared behavior of the strong interactions. Knowing the behavior of the Bethe-Salpeter kernel near its singular surfaces in momentum-space would provide a great deal of information about the nature of confinement and the properties of the resulting bound states. Our findings provide a significant step towards understanding the relation between singularities in the 't Hooft model and singularities in the $3+1$ dimensional world. Although our methods apply only to the singularities of finite processes (i.e., finite loop diagrams and truncated operator product expansions), we point out that the singularities of the exact Bethe-Salpeter kernel for the massless 't Hooft model do in fact satisfy the planar light-cone conditions. It is reasonable to expect that the same might hold true for the exact angle-integrated Bethe-Salpeter kernel in the $3+1$ dimensional case. Although the functional form of the singularities of the kernel are not known, our results indicate the probable location of these singularities and this information should be quite important in any attempt to build realistic empirical models of confinement in the relativistic system.

Acknowledgements

The author would like to thank Andrew Lesniewski for numerous discussions on the theory of Landau singularities and Howard Georgi for his guidance throughout all stages of this project.

References

- [1] G. 't Hooft, Nucl. Phys. B75 (1974) 461.
- [2] R. Chisholm, Proc. Camb. Phil. Soc. 48, (1952) 300.
- [3] G. Tiktopoulos, Phys. Rev. 131, (1963) 480.

[4] V. Novikov, M. Shifman, A. Vainshtein, V. Zakharov, Nucl. Phys. B174 (1980) 378.

Figure 1: A general 1PI diagram for quark-antiquark scattering.

Figure 2: An example of a two-loop planar diagram.

Figure 1

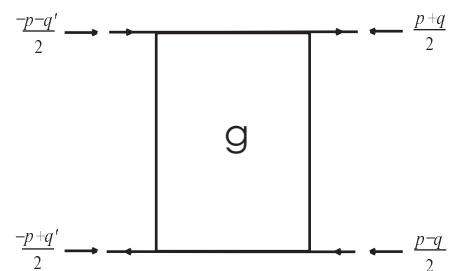


Figure 2

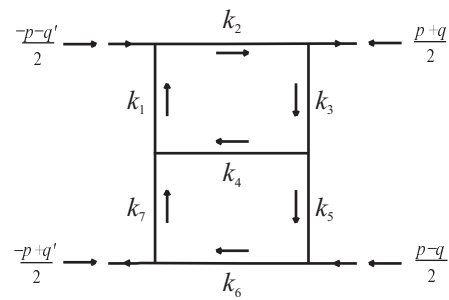


Figure 2(a-d): All possible left-to-right paths.

Figure 2(a)

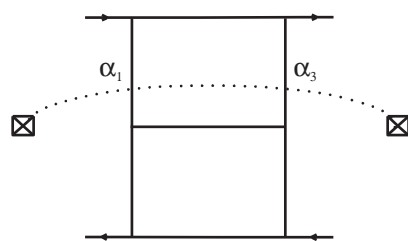


Figure 2(b)

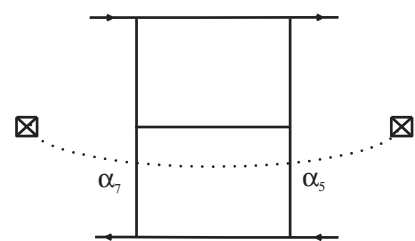


Figure 2(c)

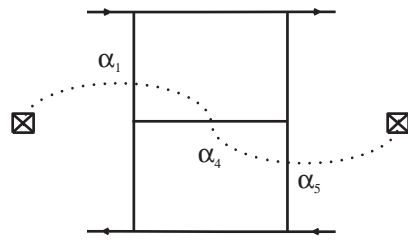


Figure 2(d)

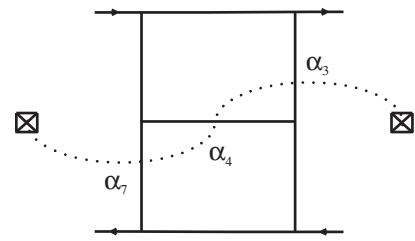


Figure 3(a-b): An example of the single/double arrow notation.

Figure 3(a)

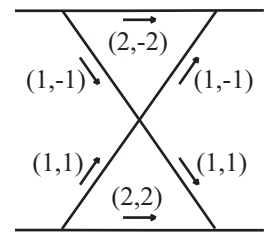


Figure 3(b)

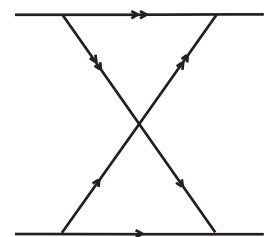


Figure 4(a-h): All possible arrangements of connected components of doubly-contracted diagrams.

Figure 4(a)

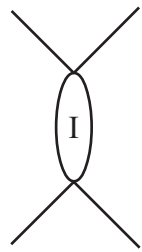


Figure 4(b)

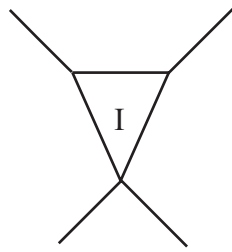


Figure 4(c)

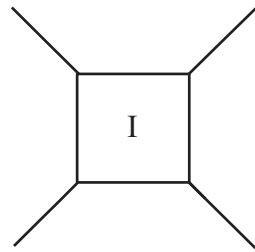


Figure 4(d)

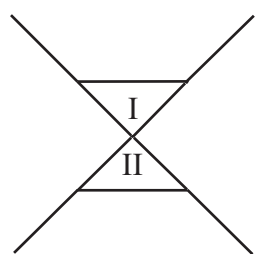


Figure 4(e)

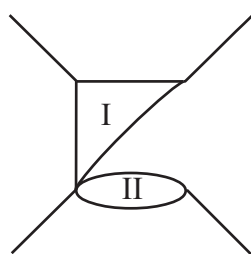


Figure 4(f)

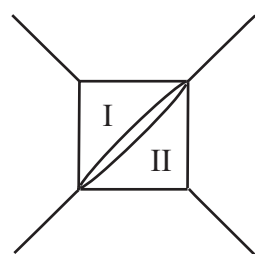


Figure 4(g)

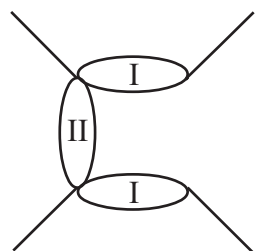


Figure 4(h)

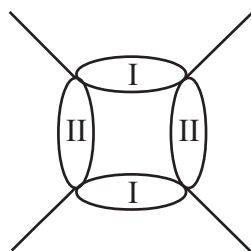


Figure 5(a-b): An example of a connected diagram involving the gluon condensate.

Figure 5(a)

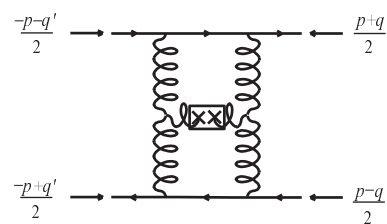


Figure 5(b)

